Atmospheric and Oceanic Science Letters xxx (xxxx) xxx

KeAi CHINESE ROOTS GLOBAL IMPACT

Contents lists available at ScienceDirect

Atmospheric and Oceanic Science Letters

journal homepage: http://www.keaipublishing.com/en/journals/atmospheric-and-oceanic-science-letters/

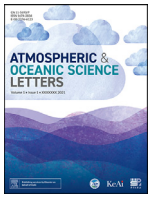

The evolving distribution of humidity conditional on temperature and implications for compound heat extremes across China in a warming world

Caixia Liang [a], Jiacan Yuan [a,b,*]

[a] Department of Atmospheric and Oceanic Sciences & Institute of Atmospheric Sciences & Shanghai Key Laboratory of Ocean–Land–Atmosphere Boundary Dynamics and Climate Change, Fudan University, Shanghai, China
[b] Shanghai Frontiers Science Center of Atmosphere–Ocean Interaction, Fudan University, Shanghai, China

ARTICLE INFO

Keywords:
Global warming
Conditional distribution of dew point on temperature
Non-crossing quantile smoothing spline model
Compound heat extremes

关键词:
全球变暖
湿度随温度的条件概率密度分布
非交叉分位数平滑样条模型
温湿复合极端事件

ABSTRACT

The likelihood of extreme heat occurrence is continuously increasing with global warming. Under high temperatures, humidity may exacerbate the heat impact on humanity. As atmospheric humidity depends on moisture availability and is constrained by air temperature, it is important to project the changes in the distribution of atmospheric humidity conditional on air temperature as the climate continuously warms. Here, a non-crossing quantile smoothing spline is employed to build quantile regression models emulating conditional distributions of dew point (a measure of humidity) on local temperature evolving with escalating global mean surface temperature. By applying these models to 297 weather stations in seven regions in China, the study analyzes historical trends of humid-heat and dry-hot days, and projects their changes under global warming of 2.0°C and 4.5°C. In response to global warming, rising trends of humid-heat extremes, while weakening trends of dry-hot extremes, are observed at most stations in Northeast China. Additionally, results indicate an increasing trend in dry-hot extremes at numerous stations across central China, but a rise in humid-heat extremes over Northwest China and coastal regions. These trends found in the current climate state are projected to intensify under 2.0°C and 4.5°C warming, possibly influenced by the heterogeneous variations in precipitation, soil moisture, and water vapor fluxes. Requiring much lower computational resources than coupled climate models, these quantile regression models can further project compound humidity and temperature extremes in response to different levels of global warming, potentially informing the risk management of compound humid-heat extremes on a local scale.

摘要

本研究利用非交叉分位数平滑样条, 对中国七个气候分区的297个气象站分别建立了分位数回归模型, 模拟露点温度基于局地温度的条件概率密度分布对全球变暖的响应, 并预测了这些分布分别在2.0°C和4.5°C温升情景下的变化. 结果表明, (1) 这些分布对全球变暖的响应存在较大的区域异质性: 东北地区, 西北地区与沿海地区大多数站点呈现出极端湿热事件增加的趋势; 而中国中部地区的多个站点呈现出极端干热事件增加的趋势. (2) 这些趋势预计在2.0°C和4.5°C的温升情景下将进一步加剧.

1. Introduction

Multiple lines of evidence show that the increase in global mean temperature induced by human activities has exceeded 1.1°C with respect to the pre-industrial level, resulting in an increase in the frequency and intensity of extreme heat events (IPCC, 2023). Growing attention has been paid to compound weather extremes combining humidity and temperature owing to their increasing frequency of occurrence (Li et al., 2020b; Meng et al., 2022; Li et al., 2023). The changes of both dry-hot and humid-heat events are expected to have a profound impact on human health and ecosystems. On the one hand, higher humidity may superimpose on the influence of high temperatures on human health (Mora et al., 2017; Liang et al., 2024). On the other hand, compound dry-hot extremes significantly affect crop yields and enhance the frequency of wildfires (Feng et al., 2019; Dong et al., 2021).

The majority of studies on heat stress use a univariate metric to measure the combined effects of temperature and humidity (e.g., Masterton and Richardson, 1979; Rothfusz, 1990; Chen et al., 2022). However, the univariate approach is not capable of capturing the joint distribution between temperature and humidity as well as their dependence, which is important for understanding the bivariate distribution of temperature and humidity, especially for their tail distributions (McKinnon and Poppick, 2020; Yuan et al., 2020). Besides, some studies have taken a dynamical systems approach to examine the coupling

* Corresponding author.
E-mail address: jcyuan@fudan.edu.cn (J. Yuan).

https://doi.org/10.1016/j.aosl.2025.100596
Received 19 November 2024; Revised 31 December 2024; Accepted 24 January 2025
Available online xxx

Please cite this article as: C. Liang and J. Yuan, The evolving distribution of humidity conditional on temperature and implications for compound heat extremes across China in a warming world, Atmospheric and Oceanic Science Letters, https://doi.org/10.1016/j.aosl.2025.100596

strength between the temperatures and humidity involved in compound humid-heat events (Guo et al., 2022a, 2022b). Conventional methods for evaluating extreme events typically assume that the tail of the distribution for the contributing variable remains constant, while only the parameters (e.g., mean, standard deviation, etc.) change as the climate warms (e.g., Kharin et al., 2013; Kodra and Ganguly, 2014). However, the distributions of these contributing variables generally neither adhere to a standard distribution, nor are stationary as the climate gets warmer. Here, we employ a quantile regression approach to develop statistical models that capture the joint distribution between temperature and humidity, as well as its evolution under climate warming, without any assumptions about the distribution. Quantile regression is a widely employed method that effectively quantifies the impact of covariates on a specific quantile of a distribution, which is particularly useful in analyzing temporal trends in the distribution of climate variables like daily temperature and precipitation (Koenker and Bassett, 1978; Tan, 2019; Yuan et al., 2020; McKinnon and Poppick, 2020). Additionally, quantile regression models are much more computationally efficient than coupled global climate models, and allow a full coverage of the uncertainties by producing probabilistic distributions of contributing variables (Tebaldi and Knutti, 2007; Yuan et al., 2020).

China, with its large population and rapid economic growth, shows significant climatic diversity due to its vast territory and complex terrain. Recently, China has witnessed numerous compound extremes combining temperature and humidity, significantly impacting the lives of citizens (Ding and Ke, 2015; Li et al., 2020a). Additionally, the regional climate changes display large spatial heterogeneity, e.g., the noteworthy trend of warming and wetting in Northwest China (Shi et al., 2007; Wang et al., 2020). However, the conditional distribution of humidity on temperature in different climate zones of China, as well as its evolution as climate warms, remains unclear.

This study develops quantile regression models to simulate the evolving distributions of humidity conditional on temperature across different climate zones of China, as well as their anticipated patterns in a warming climate. Besides, the changes in compound humid-heat and dry-hot extremes are projected accordingly based on the tail distributions under different levels of global warming.

2. Data and methods

2.1. Data

The observational data for temperature and humidity are from the Hadley Center Integrated Surface Database v3.3.0.2022f (HadISD v3.3.0.2022f) developed by the UK Met Office, based on NOAA NCEI's Integrated Surface Database (Smith et al., 2011; Dunn et al., 2012, 2014, 2016; Dunn, 2019). We employ dew point as a measure of humidity, which is the temperature at which a given volume of air needs to be cooled at constant pressure to become saturated with water vapor. Dew point is used in this study because (1) it can be directly measured by meteorological stations, (2) it directly links to the amount of moisture in the air (as the dew point increases, the humidity of the air rises accordingly), and (3) unlike relative humidity, which must be considered alongside temperature to assess thermal comfort, the dew point—representing ambient humidity (q) through its saturation temperature—provides a more direct indication of thermal comfort (McKinnon and Poppick, 2020; Scheff and Burroughs, 2023). The daily mean temperature and dew point are calculated from the hourly data. Our analysis focuses on the summer, i.e., JJA (June–July–August), during the period between 1979 and 2022. To ensure a sufficient coverage of data, we select stations that have data available for at least 80 % of the time during 1979–2022 and cover both the first and last three years of the period. A total of 297 stations across China were selected. According to the climatic zones defined by Zhao (1983), China is divided into seven regions based on climatological temperature and aridity (Fig. 1(a)). There are a sufficient number of stations located in each region, with more stations concentrated in sub-regions over eastern China (Table S1).

The smoothed global mean temperature anomaly (GMTA) dataset is based on the Berkeley Earth Surface Temperature database (Rohde et al., 2013). Anomalies in GMTA are calculated by removing the average across 1979–2022. Then, the smoothed GMTA is obtained by applying a third-order Butterworth low-pass filter with a cutoff frequency of 1/10 years to the raw GMTA data.

To understand the causes of the variability in the distribution of dew point, this study uses ERA5 variables for analysis, including the monthly mean total precipitation, soil moisture, specific humidity, wind, and vertical integral of divergence of moisture flux, which are produced by ECMWF (the European Centre for Medium-Range Weather Forecasts) (Hersbach et al., 2023a, 2023b).

2.2. Quantile smoothing splines

We develop quantile regression models at each station using non-crossing quantile smoothing splines to assess the alterations in the distribution of dew point conditional on the co-occurring local temperature and GMTA (McKinnon and Poppick, 2020). For a given quantile τ, the dew point on day t is modeled as

$$T_{\mathrm{d}}{}'_{\tau}(t) = s_{0,\tau}\left(T'(t)\right) + \beta_{1,\tau}G'(t) + G'(t)s_{1,\tau}\left(T'(t)\right) + \beta_{0,\tau}, \quad (1)$$

where $T'(t)$ is the co-occurring local temperature and $G'(t)$ is the smoothed GMTA. Both $s_{0,\tau}$ and $s_{1,\tau}$ are functions of $T'(t)$, indicating regularized quantile smoothing splines that capture the potentially nonlinear relationship between $T_{\mathrm{d}}{}'_{\tau}(t)$ and $T'(t)$. $\beta_{0,\tau}$ is the intercept of the model, while $\beta_{1,\tau}$ is the parameter that characterizes the relationship between dew point temperature and G'(t). The first three terms on the right-hand side of Eq. (1) represent the changes in $T_{\mathrm{d}}{}'_{\tau}(t)$ that depend on the $T'(t)$, $G'(t)$, and interactions between $T'(t)$ and $G'(t)$. The combined second and third terms of Eq. (1) indicate the change in $T_{\mathrm{d}}{}'_{\tau}(t)$ per 1°C increase in GMTA, at a station with a local temperature anomaly of $T'(t)$. A regularization parameter is used to control the complexity of the spline, which is measured by the number of active knots. The parameter is selected through minimization of a high-dimensional Bayesian Information Criterion. Non-crossing constraints are applied during the fitting procedure to avoid the dew point temperature exceeding the temperature and the low quantile exceeding the high quantile. From each of the seven climate zones, we selected a station to develop quantile regression models as an example (Fig. S1). The joint distribution between T' and $T_{\mathrm{d}}{}'$ exhibits distinct patterns in different climate zones, indicating varying responses of atmospheric moisture to changes in local temperature under different climate conditions (Fig. S1, colored hexagons). The quantile of $T_{\mathrm{d}}{}'$ conditional on T' developed by the quantile regression model can skillfully capture the joint distribution between T' and $T_{\mathrm{d}}{}'$. The 5th quantile and 95th quantile of $T_{\mathrm{d}}{}'$ respond differently to GMTA during high local temperatures (95th quantile) across regions. We applied the same analysis on all the selected stations over the period from 1979 to 2022, and calculated the T_{d} change rate, i.e., changes in $T_{\mathrm{d}}{}'_{5,T'95}$ and $T_{\mathrm{d}}{}'_{95,T'95}$ per 1°C increase in GMTA, to explore the changes in extremely high and low dew points conditional on high temperature in the context of global warming. We also tried other thresholds to identify the extremely dry or humid condition (e.g., $T_{\mathrm{d}}{}'_{10}$ or $T_{\mathrm{d}}{}'_{90}$), and found that the results are insensitive to the adjustment of the threshold (Fig. S2).

2.3. Future projection

Based on the quantile regression model in Eq. (1), we project the distribution of dew point conditional on temperature across China at different levels of global warming. Our analysis focuses on the warming levels of 2.0°C and 4.5°C, corresponding to the temperature target set by the Paris Agreement and the projected global mean temperature increase by 2100 under fossil-fuel intensive scenarios, respectively. The

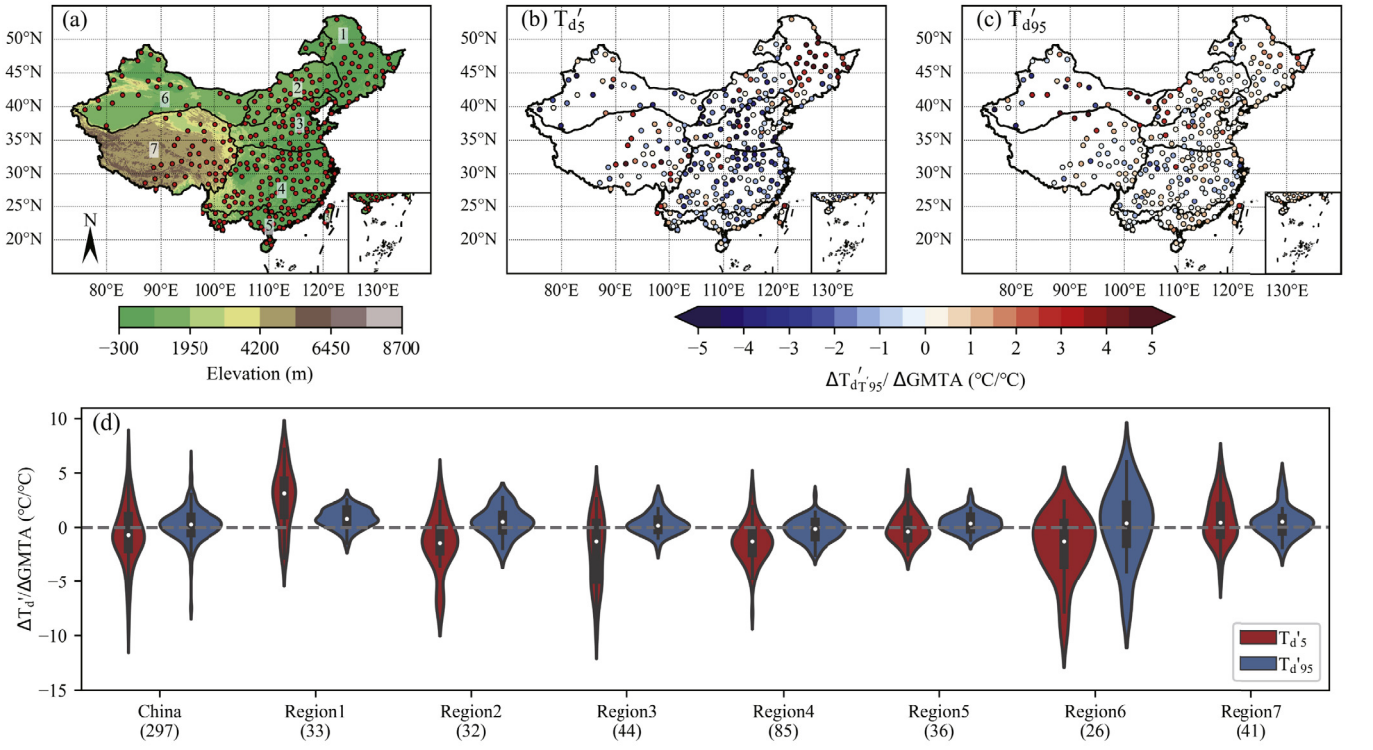

Fig. 1. (a) Map of elevation, distribution of meteorological stations, and regions of climate zones in China. Numbers on the map mark the seven climate zones, respectively. (b) Spatial distribution of the estimated T_d change rate in $T_d'_{5,T'95}$ at selected HadISD stations across China. (c) The same as (b) but for $T_d'_{95,T'95}$. (d) Violin plot of the T_d change rate in $T_d'_{5,T'95}$ and $T_d'_{95,T'95}$ at stations across China and in seven regions.

$G'(t)$ corresponding to the two warming levels was calculated relative to the 1850–1900 baseline of GMTA and used as the input to estimate the projected dew point under these warming scenarios. It should be noted that, in the future projection, the extremely high local temperature is fixed at the 95th percentile in the historical period, so that the results reveal what extreme conditions of humidity people in a warming future will experience even at the same high temperature as the current climate.

3. Results

In response to global warming, except for region 1 and region 7, a reduction in the 5th percentile of dew point conditional on high temperature is observed over most regions (Fig. 1(b)). This indicates that dry-hot days get drier when the climate gets warmer, which shares some consistency with findings in previous studies (Feng and Fu, 2013; Huang et al., 2016). However, the T_d change rates in the 95th percentile are negligible except for some stations over Northwest and Northeast China. This may be attributable to the fact that, in humid climates, the 95th percentile of dew point is very close to the air temperature, limiting its increase since the dew point cannot exceed the air temperature (Fig. 1(c)). Many stations in Northwest China show increases in the T_d change rate in $T_d'_{95,T'95}$, suggesting that climate warming may exacerbate the humid-heat situation in the region.

From the violin plot of the T_d change rate distribution (Fig. 1(d)), drying trends of dry-hot days are observed over 50 % of stations in China, while most of them are from regions 2–6. In region 1, the T_d change rates are positive at over 85 % of stations on dry-hot days and at over 82 % of stations on humid-heat days, indicating a reduction of dry-hot extremes and an enhancement of humid-heat extremes over this region. Besides region 1, the T_d change rates on humid-heat days are positive at over 50 % of stations in regions 2, 5, 6, and 7, indicating elevated humidity of humid-heat extremes in response to global warming. In summary, the T_d change rate is negative on dry-hot days and positive on humid-heat days at >50 % of stations across China, and in regions 2, 5, and 6, indicating an increase in the intensity of extreme dry-hot and extreme humid-heat events over these regions.

Based on the models developed at each station, we project the distribution of dew point conditional on hot days across China under global warming of 2.0°C and 4.5°C (Fig. 2). The result shows that the distribution of $T_d'_{5,T'95}$ at stations across China reveals a pronounced boundary. The boundary approximately coincides with the Heihe-Tengchong Line, which is a significant geographical demarcation in China that highlights the stark disparity in population (Hu, 1935). The $T_d'_{5,T'95}$ is positive at all stations east of the Heihe-Tengchong Line, while it is either close to or below zero at stations west of the line under 2.0°C warming (Fig. 2(a)). Under 4.5°C warming, the contrast in $T_d'_{5,T'95}$ between stations east and west of the Heihe-Tengchong Line is increased (Fig. 2(c)). The $T_d'_{95,T'95}$ is positive at all stations under 2°C warming, while it is positive at most stations under 4.5°C warming, except for a few stations in region 6 (Fig. 2(b, d)). The $T_d'_{95,T'95}$ at stations in eastern China is generally likely to exceed 24°C, with some stations in southern China exceeding 30°C (Fig. 2(d), Table S2).

We further investigate the projected changes in $T_d'_{5,T'95}$ and $T_d'_{95,T'95}$ under global warming of 2.0°C and 4.5°C, compared with the present climate (2003–2022). Under 2.0°C warming, $T_d'_{5,T'95}$ is projected to increase at most stations in region 1 and 7, where the highest increase is about 6°C. At stations in the remaining regions, $T_d'_{5,T'95}$ is projected to decrease, with the largest drop being below 8°C (Fig. 3(a)). These features of changes in $T_d'_{5,T'95}$ are maintained under global warming of 4.5°C (Fig. 3(c)), except that the changes are more pronounced in magnitude. For $T_d'_{95,T'95}$, the changes are negligible from the present climate to a warming level of 2°C, while they are more pronounced from the present climate to a warming level of 4.5°C. The distributions of changes in $T_d'_{5,T'95}$ and $T_d'_{95,T'95}$ across stations over China and regions further confirm that the direction of changes

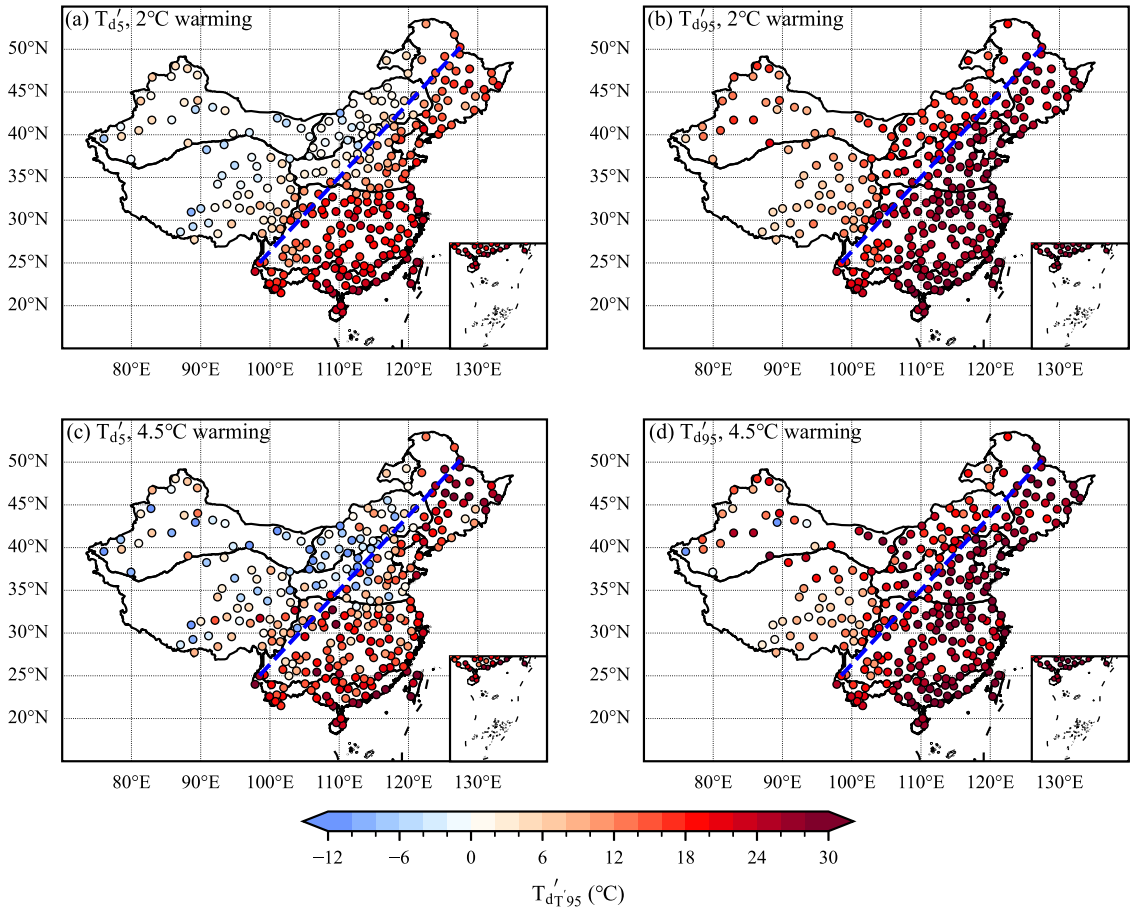

Fig. 2. Projected spatial distribution of $T_d'_{5,T'95}$ and $T_d'_{95,T'95}$ under (a, b) 2.0°C warming and (c, d) 4.5°C warming, respectively. The blue dashed line is the Heihe-Tengchong Line.

under 2°C warming is consistent with that under 4.5°C warming, except that the magnitudes are much larger in the latter than in the former (Fig. 3(e, f)).

4. Discussion and conclusions

This study used the non-crossing quantile smoothing splines model to simulate the distribution of dew point conditional on local temperature, as well as their evolution accompanied by GMTA, without any assumptions about the distribution. In addition, the T_d change rates of $T_d'_{5,T'95}$ and $T_d'_{95,T'95}$ were calculated to project the changes in the tail distribution of dew point on hot days under global warming. Results showed that, in general, the changes in the low tail of dew point conditional on high local temperature are more sensitive to global warming than those in the high tail. The T_d change rates are spatially heterogeneous across the seven climate regions of China. Positive T_d change rates can be seen on both hot-humid days and dry-hot days in region 1, indicating a reduction of dry-hot days and enhancement of humid-heat days over Northeast China. The T_d change rates are generally negative on dry-hot days in regions 2–6, whereas they are predominantly positive on hot-humid days in regions 2, 5, 6, and 7, indicating amplifications of dry-hot days and humid-heat days due to changes in the atmospheric moisture content. As the climate gets warmer, the low tails of T_d conditional on high local temperature are positive at stations east of the Heihe-Tenchong Line, and negative at stations west of the line. The high tails of T_d conditional on high local temperature are positive at nearly all stations, with maximum values exceeding 30°C over the east of China and gradually decreasing towards the west. The changes of T_d from the current climate state to future global warming are consistent with the distribution of the T_d change rate in the current period in each region, except for the intensity in the magnitude of changes. Global warming tends to elevate the intensity of dry-hot extremes at numerous stations in Central China, and intensifies humid-heat extremes at some stations over Northwest China and coastal regions of China.

The potential mechanisms behind the different responses in the distribution of dew point conditional on local high temperature to global warming were also explored. For dry-hot days, the negative T_d change rate in regions 2–6 may be due to the decreasing trends in total precipitation and soil moisture (Fig. S3(a, b)). Reduced precipitation will result in decreased soil moisture, which in turn reduces soil evaporation and ultimately weakens atmospheric moisture. The positive T_d change rate on humid-heat days at stations in the Qinghai–Tibet Plateau and coastal areas may be due to the increase in moisture transport and moisture convergence of moisture flux over the corresponding regions under global warming (Fig. S3(c)). Although not significant, weak positive trends in both precipitation and soil moisture are observed over the eastern part of Northeast China. However, studies show that extreme summer rainfall in Northeast China has increased, and is projected to rise further (Meng et al., 2024; Xie et al., 2024). Additionally, more than half of the stations in Northwest China exhibit a positive trend in the T_d change rate on humid-heat days, which may be explained by the increased moisture flux and significant convergence of moisture flux over these areas (Fig. S3(c)). Previous studies found a humidification trend in Northwest China during recent decades (Shi et al., 2007; Wang et al., 2020), with a focus on changes in precipitation. This study provides a new perspective from the humidity conditional on high-temperature days, indicating a risk of increasing the humid-heat situation in Northwest China.

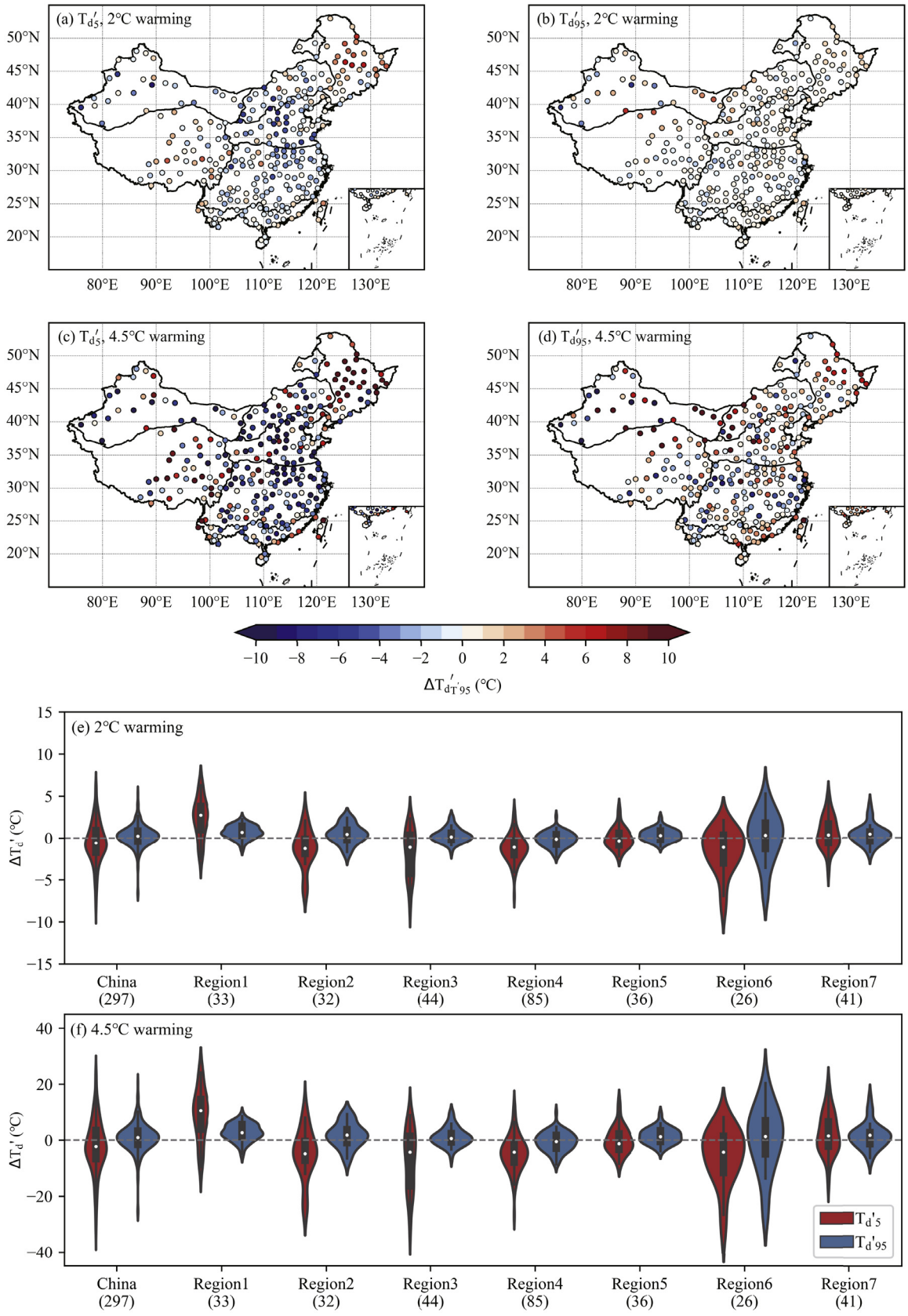

Fig. 3. Spatial pattern of changes in the 5th and 95th percentiles of dew point temperature conditional on high temperature from the present day (2003–2022) to (a, b) 2.0°C and (c, d) 4.5°C warming. (e, f) The same as Fig. 2(d) but for changes in $T_d'_{5,\,T'95}$ and $T_d'_{95,\,T'95}$ from the present day to (e) 2°C and (f) 4.5°C warming.

The results of the non-crossing quantile smoothing splines model show good consistency with the characteristics of compound event variations detected by conventional approaches (Fig. S4), demonstrating its ability to effectively capture variations of tail distributions of T_d conditional on temperature during the historical period. The model's advantage lies in its ability to project future changes in the joint distribution without assuming a prescribed distribution, while significantly reducing the computational demand compared to climate model simulations. The projected results highlight key regions where compound humid-heat/dry-hot extremes may increase dramatically under different levels of global warming. This potentially provides information for the risk management of compound heat extremes on a local scale.

Funding

This research was supported by the National Natural Science Foundation of China [grant number 42175066] and the Shanghai International Science and Technology Partnership Project [grant number 21230780200].

Supplementary materials

Supplementary material associated with this article can be found, in the online version, at doi:10.1016/j.aosl.2025.100596.

References

Chen, H., He, W., Sun, J., Chen, L., 2022. Increases of extreme heat-humidity days endanger future populations living in China. Environ. Res. Lett. 17 (6), 064013. doi:10.1088/1748-9326/ac69fc.

Ding, T., Ke, Z., 2015. Characteristics and changes of regional wet and dry heat wave events in China during 1960–2013. Theor. Appl. Climatol. 122 (3), 651–665. doi:10.1007/s00704-014-1322-9.

Dong, L., Leung, L.R., Qian, Y., Zou, Y., Song, F., Chen, X., 2021. Meteorological environments associated with California wildfires and their potential roles in wildfire changes during 1984–2017. J. Geophys. Res. Atmos. 126 (5), e2020JD033180. doi:10.1029/2020JD033180.

Dunn, R.J.H., 2019. HadISD Version 3: Monthly Updates. Hadley Centre Technical Note HCTN 072-103, pp. 1–10. https://digital.nmla.metoffice.gov.uk/digitalFile_13890750-fb6f-42c7-92df-1c4504621fae/.

Dunn, R.J.H., Willett, K.M., Morice, C.P., Parker, D.E., 2014. Pairwise homogeneity assessment of HadISD. Clim. Past 10 (4), 1501–1522. doi:10.5194/cp-10-1501-2014.

Dunn, R.J.H., Willett, K.M., Parker, D.E., Mitchell, L., 2016. Expanding HadISD: Quality-controlled, sub-daily station data from 1931. Geosci. Instrum. Methods Data Syst. 5 (2), 473–491. doi:10.5194/gi-5-473-2016.

Dunn, R.J.H., Willett, K.M., Thorne, P.W., Woolley, E.V., Durre, I., Dai, A., Parker, D.E., Vose, R.S., 2012. HadISD: A quality-controlled global synoptic report database for selected variables at long-term stations from 1973 to 2011. Clim. Past 8 (5), 1649–1679. doi:10.5194/cp-8-1649-2012.

Feng, S., Fu, Q., 2013. Expansion of global drylands under a warming climate. Atmos. Chem. Phys. 13 (19), 10081–10094. doi:10.5194/acp-13-10081-2013.

Feng, S., Hao, Z., Zhang, X., Hao, F., 2019. Probabilistic evaluation of the impact of compound dry-hot events on global maize yields. Sci. Total Environ. 689, 1228–1234. doi:10.1016/j.scitotenv.2019.06.373.

Guo, Y., Huang, Y., Fu, Z., 2022a. Regional compound humidity-heat extremes in the mid-lower reaches of the Yangtze river: A dynamical systems perspective. Environ. Res. Lett. 17 (6), 064032. doi:10.1088/1748-9326/ac715f.

Guo, Y., Huang, Y., Fu, Z., 2022b. What causes compound humidity-heat extremes to have different coupling strengths over the mid-lower reaches of the Yangtze River? Clim. Dyn. 60, 4099–4109. doi:10.1007/s00382-022-06532-6.

Hersbach, H., Bell, B., Berrisford, P., Biavati, G., Horányi, A., Muñoz Sabater, J., Nicolas, J., et al., 2023a. ERA5 monthly averaged data on pressure levels from 1940 to present. Copernicus Climate Change Service (C3S) Climate Data Store (CDS). doi:10.24381/cds.6860a573.

Hersbach, H., Bell, B., Berrisford, P., Biavati, G., Horányi, A., Muñoz Sabater, J., Nicolas, J., et al., 2023b. ERA5 monthly averaged data on single levels from 1940 to present. Copernicus Climate Change Service (C3S) Climate Data Store (CDS). doi:10.24381/cds.f17050d7.

Hu, H., 1935. The distribution of population in China, with statistics and maps. Acta Geogr. Sin. 2 (2), 33–74. doi:10.11821/xb193502002.

Huang, J., Yu, H., Guan, X., Wang, G., Guo, R., 2016. Accelerated dryland expansion under climate change. Nat. Clim. Chang. 6 (2), 166–171. doi:10.1038/nclimate2837.

IPCC, 2023. Climate Change 2023: Synthesis Report. In: Contribution of Working Groups I, II and III to the Sixth Assessment Report of the Intergovernmental Panel On Climate Change [Core Writing Team, H. Lee and J. Romero (eds.)]. IPCC, Geneva, Switzerland, pp. 35–115. doi:10.59327/IPCC/AR6-9789291691647.

Kharin, V.V., Zwiers, F.W., Zhang, X., Wehner, M., 2013. Changes in temperature and precipitation extremes in the CMIP5 ensemble. Clim. Chang. 119 (2), 345–357. doi:10.1007/s10584-013-0705-8.

Kodra, E., Ganguly, A.R., 2014. Asymmetry of projected increases in extreme temperature distributions. Sci. Rep. 4, 5884. doi:10.1038/srep05884.

Koenker, R., Bassett, G., 1978. Regression quantiles. Econometrica 46 (1), 33. doi:10.2307/1913643.

Li, C., Sun, Y., Zwiers, F., Wang, D., Zhang, X., Chen, G., Wu, H., 2020a. Rapid warming in summer wet bulb globe temperature in China with Human-induced climate change. J. Clim. 33 (13), 5697–5711. doi:10.1175/JCLI-D-19-0492.1.

Li, D., Yuan, J., Kopp, R.E., 2020b. Escalating global exposure to compound heat-humidity extremes with warming. Environm. Res. Lett. 15 (6), 064003. doi:10.1088/1748-9326/ab7d04.

Li, W., Sun, B., Wang, H., Zhou, B., Li, H., Xue, R., Duan, M., Luo, X., Ai, W., 2023. Anthropogenic impact on the severity of compound extreme high temperature and drought/rain events in China. NPJ. Clim. Atmos. Sci. 6 (1), 1–13. doi:10.1038/s41612-023-00413-3.

Liang, C., Yuan, J., Tang, X., Kan, H., Cai, W., Chen, J., 2024. The influence of humid heat on morbidity of megacity Shanghai in China. Environ. Int. 183, 108424. doi:10.1016/j.envint.2024.108424.

Masterton, J.M., Richardson, F., 1979. Humidex: A method of quantifying human discomfort due to excessive heat and humidity. Environment Canada, Downsview, Ontario, Canada, pp. 35–36.

McKinnon, K.A., Poppick, A., 2020. Estimating changes in the observed relationship between humidity and temperature using noncrossing quantile smoothing splines. J. Agric. Biol. Environ. Stat. 25 (3), 292–314. doi:10.1007/s13253-020-00393-4.

Meng, F., Xie, K., Liu, P., Chen, H., Wang, Y., Shi, H., 2024. Extreme precipitation trends in Northeast China based on a non-stationary generalized extreme value model. Geosci. Lett. 11 (1), 13. doi:10.1186/s40562-024-00331-z.

Meng, Y., Hao, Z., Feng, S., Zhang, X., Hao, F., 2022. Increase in compound dry-warm and wet-warm events under global warming in CMIP6 models. Glob. Planet. Chang. 210, 103773. doi:10.1016/j.gloplacha.2022.103773.

Mora, C., Dousset, B., Caldwell, I.R., Powell, F.E., Geronimo, R.C., Bielecki, C.R., Counsell, C.W.W., et al., 2017. Global risk of deadly heat. Nat. Clim. Chang. 7 (7), 501–506. doi:10.1038/nclimate3322.

Rohde, R., Curry, J., Groom, D., Jacobsen, R., Muller, R.A., Perlmutter, S., Rosenfeld, A., Wickham, C., Wurtele, J., 2013. Berkeley earth temperature averaging process. Geoinfor. Geostat.: An overview 1 (2), 1–13. doi:10.4172/gigs.1000103.

Rothfusz, L.P., 1990. The heat index "equation" (or, more than you ever wanted to know about heat index). Technical attachment, SR/SSD 90–23. Available at: https://www.weather.gov/media/ffc/ta_htindx.PDF.

Scheff, J., Burroughs, J.C., 2023. Diverging trends in US summer dewpoint since 1948. Int. J. Climatol. 43 (9), 4183–4195. doi:10.1002/joc.8081.

Shi, Y., Shen, Y., Kang, E., Li, D., Ding, Y., Zhang, G., Hu, R., 2007. Recent and future climate change in Northwest China. Clim. Chang. 80 (3–4), 379–393. doi:10.1007/s10584-006-9121-7.

Smith, A., Lott, N., Vose, R., 2011. The integrated surface database: Recent developments and partnerships. Bull. Am. Meteorol. Soc. 92 (6), 704–708. doi:10.1175/2011BAMS3015.1.

Tan, X., 2019. Modeling distributional changes in winter precipitation of Canada using bayesian spatiotemporal quantile regression subjected to different teleconnections. Clim. Dyn. 52, 2105–2124. doi:10.1007/s00382-018-4241-0.

Tebaldi, C., Knutti, R., 2007. The use of the multi-model ensemble in probabilistic climate projections. Philos. Transact. Royal Soc. London A: Math. Phys. Eng. Sci. 365 (1857), 2053–2075. doi:10.1098/rsta.2007.2076.

Wang, Q., Zhai, P.-M., Qin, D.-H., 2020. New perspectives on 'warming–wetting' trend in Xinjiang, China. Adv. Clim. Chang. Res. 11 (3), 252–260. doi:10.1016/j.accre.2020.09.004.

Xie, Z., Fu, Y., He, H.S., Wang, S., Wang, L., Liu, C., 2024. Increases in extreme precipitation expected in Northeast China under continued global warming. Clim. Dyn. 62 (6), 4943–4965. doi:10.1007/s00382-024-07144-y.

Yuan, J., Stein, M.L., Kopp, R.E., 2020. The evolving distribution of relative humidity conditional upon daily maximum temperature in a warming climate. J. Geophys. Res. Atmos. 125 (19). doi:10.1029/2019JD032100.

Zhao, S., 1983. A new scheme for comprehensive physical regionalization in China. Acta Geogr. Sin. 38 (1), 1–10 doi:10.11821/xb198301001. (In Chinese).